

MECHANISM FOR TRANSITION TO TURBULENCE IN BUOYANT PLUME FLOW

SHIGEO KIMURA and ADRIAN BEJAN

Department of Mechanical Engineering, Campus Box 427,
University of Colorado, Boulder, CO 80309, U.S.A.

(Received 21 July 1982 and in final form 25 January 1983)

Abstract—This paper reports a theoretical and experimental study of the fundamental mechanism responsible for transition in natural convection plume flow. Theoretically, it is argued that the transition occurs when the time of viscous penetration normal to the plume becomes comparable with the minimum time period with which the plume can fluctuate as an unstable inviscid stream. It is also argued that at transition the plume wavelength must always scale with the local plume diameter. The experimental part of the study focused on transition in the axisymmetric air plume above a point heat source. Smoke visualization of the plume shape at transition led to extensive observations that support strongly the transition mechanism proposed theoretically. The transitional plume is seen to meander in a plane (two-dimensionally) and with a wavelength which scales with the plume diameter. If excited externally by many such wavelengths, the plume has the property to select the natural wavelength proposed theoretically. The equivalence between the present transition mechanism and the transition predicted by the buckling theory is discussed.

NOMENCLATURE

D	local plume diameter [m]
f	disturbance frequency [s^{-1}]
g	gravitational acceleration [$m\ s^{-2}$]
H	loudspeaker height [m]
k	thermal conductivity [$W\ m^{-1}\ K^{-1}$]
N	ratio between t_v and t_{min} ; same as buckling number N_B [16, 21]
Q	heat input [W]
t	time [s]
t_{min}	minimum plume fluctuation time [s]
t_v	viscous communication time [s]
U	plume velocity [$m\ s^{-1}$]
x	transition height [m]

Greek symbols

α	thermal diffusivity [$m^2\ s^{-1}$]
β	thermal expansion coefficient [K^{-1}]
λ	wavelength [m]
λ_B	buckling wavelength [m]
λ_{min}	minimum plume fluctuation wavelength [m]
ν	kinematic viscosity [$m^2\ s^{-1}$]

Subscripts

B	buckling property
0	reference state

1. INTRODUCTION

THIS is a study of the fundamental mechanism which causes the transition to turbulence in buoyant plumes rising from a point heat source. The transition to turbulence is one of the most basic phenomena which is not yet fully understood. The importance of understanding this phenomenon is self-evident, considering the importance of predicting the ensuing turbulent motion of fluids. The transition phenomenon is particularly important in the field of heat transfer, environ-

mental engineering, atmospheric research, because turbulence is the most effective transport mechanism known to man.

The buoyant plume is one frequent type among the many occurrences of free-convection flows in engineering and other applications. In this paper we are specifically interested in the axisymmetric buoyant plume rising from a point heat source in a quiescent environment. Existing studies on such plumes and the plume transition phenomenon have been summarized by Gebhart [1], who showed that considerable effort has been devoted to this problem over the past few decades. For example, the laminar 2-dim. and axisymmetric plume has been studied by Yih [2, 3], and Brand and Lahey [4]. Probably the most thorough treatment of this problem is the numerical analysis by Fujii [5].

Experimental studies on the plane plume above the line source were reported by Brodowicz and Kierkus [6], Forstrom and Sparrow [7], and Schorr and Gebhart [8]. The latter two works are concerned with the plume behavior in the transition regime as well as in the laminar regime. Schorr and Gebhart observed by means of interferometric flow visualization a regular laminar 'swaying' motion at a large distance above a line heat source. This type of boundary layer swaying motion is amplified and eventually the flow becomes turbulent. Forstrom and Sparrow also observed the existence of swaying motion at a fixed point in space near transition, by means of a thermocouple placed midway between the mid-plane and the edge of the thermal boundary layer.

The theoretical research on transition in plume flow proceeded along the lines of hydrodynamic stability theory. For example, Pera and Gebhart [9] showed by integrating inviscid cases of the Orr-Sommerfeld type equation that the assumed 2-dim. plume base flow is less stable for the asymmetric mode than for the

symmetric one. A thorough study of buoyancy effect on hydrodynamic stability in the vertical round jet has been conducted by Mollendorf [10] who found that buoyancy strongly affects the stability of jets.

In the discussion of existing information on transition, the adopted theoretical view is rooted in the theory of hydrodynamic stability. This point of view consists of recognizing the existence of external disturbances of many wavelengths which, when superimposed on the laminar flow of interest, might render the flow unstable, thus triggering turbulence. The same comment applies to the existing experimental work on transition: this time the disturbances are introduced into the flow externally, for example, by using a loudspeaker. Thus, as we look back at the important advances made in this field of transition research, it is important to keep in mind that this research is not about flows alone, but about the response of certain flows to certain disturbances.

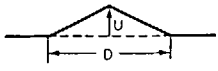
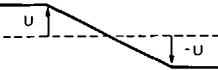
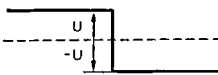
From the outset, it must be said that the point of view which stimulated the present study differs somewhat from the classical hydrodynamic stability approach. The difference lies in the fact that in this study 'transition' is viewed as an intrinsic property of the flow alone, i.e. a property which is not related to the nature or questionable presence of an external disturbance. It is shown in the next section that this intrinsic property stems from hydrodynamic stability results which have been known for one hundred years. However, it is apparent that the significance of these results *vis-à-vis* transition has not been emphasized until now.

2. THE MINIMUM WAVELENGTH FOR INVISCID FLOW INSTABILITY: TIME CRITERION FOR TRANSITION

The type of classical stability results which stimulated the present study is exhibited in Table 1. In a 1880 paper, Rayleigh [11] showed that an inviscid jet of triangular profile is unstable to disturbances whose wavelengths exceed a certain multiple of the jet thickness D . Rayleigh did not calculate explicitly the minimum wavelength of 'neutral' stability: his discussion focused primarily on another, longer wavelength ($\approx 2\frac{1}{2}D$) for which an assumed disturbance exhibits the highest amplification rate ([11], p. 65). The minimum wavelength for instability, λ_{min} , which results from Rayleigh's jet analysis is listed in row (a) of Table 1.

Similar results have been known from stability studies involving other basic flows. For example, Rayleigh considered also the free shear flow profile (b) and found instability for wavelengths greater than '5D' ([11], p. 63). Thus, for several velocity profiles of the base flow, the minimum wavelength for inviscid instability always scales with the transversal dimension of the flow. As shown in row (c) of Table 1, this scaling is consistent with another classical result, namely, the instability of a plane of velocity discontinuity to any wavelength [12]. In this case, the minimum wavelength is zero, i.e. of the same order as the shear layer thickness. The proportionality $\lambda_{min} \sim D$ is also encountered in the

Table 1. Minimum wavelength for instability in inviscid flow (after refs. [12-14])

(a) Free jet		$\lambda_{min} = 1.714 D$
(b) Shear layer		$\lambda_{min} = 4.914 D$
(c) Velocity discontinuity		$\lambda_{min} = 0 (D=0)$

stability analysis of radially symmetric flows, for example, round jets [13] and annual shear layers [14].

The object of this study is the transition to turbulence in a buoyant plume. This flow is represented approximately by profile (a) in Table 1. The theoretical basis of the present research is the idea that the $\lambda_{min} \sim D$ scaling discussed in the preceding paragraphs is an intrinsic property of the inviscid flow, and that this property is responsible for transition. The mission of the experimental work outlined later in this paper is to verify the validity of this theoretical viewpoint. Below, a simple scaling argument is offered as a basis for the transition phenomenon, and as an analytical result to be verified by experiment.

Each longitudinal length scale $\lambda (\geq \lambda_{min})$ and the plume velocity U define a new time scale,

$$t \sim \frac{\lambda}{U/2}. \tag{1}$$

This is the period in which the stream will fluctuate relative to the still environment. Note that $U/2$ is the plume mean velocity which, from symmetry considerations, represents the order of magnitude of the velocity with which the λ wave rises. The same flow is unstable to an infinity of wavelengths $\lambda > \lambda_{min}$ [11], hence, the same flow can fluctuate with an infinity of periods

$$t \geq t_{min} \sim \frac{\lambda_{min}}{U/2}. \tag{2}$$

However, since λ_{min} is proportional to D (Table 1), the minimum fluctuation period t_{min} is proportional to D also. The proportionality $t_{min} \sim D$ is shown as a straight line on Fig. 1, where D is plotted on the ordinate because in natural convection the plume becomes thicker with altitude. For any inviscid stream of thickness D , fluctuations with a period shorter than t_{min} are stable.

The issue of whether the stream (U, D) will become unstable is decided by examining the 'inviscid' of the flow. *Inviscid* or *viscid* is a flow property, not a fluid property. If the stream tends to fluctuate (wave), then plume fluid will tend to collide with the stagnant ambient intermittently, at time intervals $t > t_{min}$. The plume stream remains inviscid if during each interval t it is not overcome by viscous effects, i.e. it does not learn

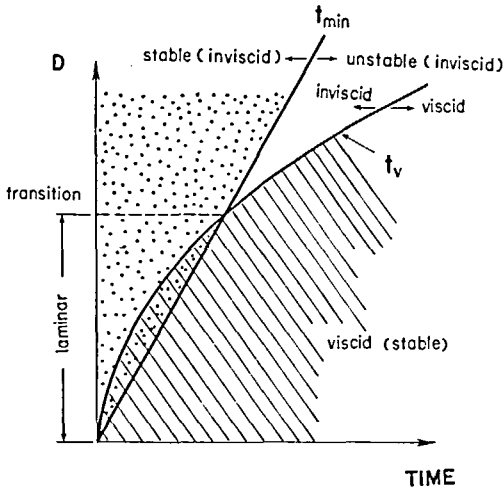


FIG. 1. The internal competition between the minimum period for inviscid instability (t_{min}) and the viscous communication time (t_v).

by viscous diffusion of the presence of a restraining ambient. The characteristic time of viscous penetration (t_v) from the plume–ambient interface to the plume centerline (over a distance of order $D/2$) is given by the classical solution to Stokes' first problem [15]

$$\frac{D/2}{2(\nu t_v)^{1/2}} \sim 1, \tag{3}$$

in other words,

$$t_v \sim \frac{D^2}{16\nu}. \tag{4}$$

Thus, at any level (height) in its development, no plume will remain inviscid forever. Figure 1 shows that if the fluctuation time exceeds the viscous penetration time t_v , the plume will remain laminar because its ambient will successfully continue to restrain it viscously.

The inviscid instability predicted by so many hydrodynamic stability studies (Table 1) is therefore possible only if t_v exceeds t_{min} . In Fig. 1, this condition corresponds to the intersection of the $t_{min} \sim D$ line with the $t_v \sim D^2$ parabola,

$$t_{min} \sim t_v. \tag{5}$$

The phenomenon of transition to non-laminar plume flow appears to be governed by the time criterion

$$O(N) = 1 \tag{6}$$

where

$$N = \frac{t_v}{t_{min}} \sim \frac{DU/\nu}{32(\lambda_{min}/D)}. \tag{7}$$

Noting that λ_{min}/D is a constant (Table 1), the $O(N) = 1$ criterion is equivalent to stating that at transition the stream (local) Reynolds number DU/ν is a certain (critical) constant considerably greater than unity. Thus, approximating $\lambda_{min} \approx 1.714D$ from Table 1, the

transition criterion (6) becomes

$$\frac{DU}{\nu} > 55, \tag{8}$$

for transition to non-laminar flow.

The object of the following experimental study is to test the validity of the $t_{min} \sim t_v$ scaling, as mechanism for transition in plume flow. It is worth noting from the outset that the theoretical time criterion is already compatible with two earlier conclusions regarding transition:

(1) Experimentally, it is a universal conclusion that transition is associated with a characteristic Reynolds constant considerably greater than unity.

(2) Theoretically, the same transition criterion is recommended by the buckling theory of inviscid jets [16], where λ_{min} is replaced by the buckling wavelength of the stream, $\lambda_B = (\pi/2)D = 1.57D$.

An important distinction must be made, however, between the above theoretical criterion [equations (6)–(8)] and the universally accepted fact that the transition is characterized by $DU/\nu = \text{constant}$. To begin with, the notion of a ‘critical’ Reynolds number of transition is of purely empirical origin. On the theoretical side, the linearized (small-disturbance) equations of hydrodynamic stability theory can easily be subjected to scale analysis to show that the Reynolds number is indeed an important dimensionless parameter; comparing the Reynolds number with unity (one), we can say whether or not the viscous terms can be neglected in the stability analysis. Note, however, that this scaling argument is not about ‘transition’, rather, it is about the simplification of stability analysis. Also on the theoretical side, the Reynolds number appears in the solution to the complete Orr–Sommerfeld equation: however, unlike in criterion (8), the stability-derived transition Reynolds number is not a constant. (It is a function of the wavelength of each postulated disturbance.)

In view of this discussion, the time criterion (6)–(8) seems to provide for the first time a hydrodynamic stability scaling basis for “the Reynolds number = a constant considerably greater than unity” as transition criterion. The experimental observations summarized later in Section 6 show that at transition the order of UD/ν is 10^2 , in agreement with the time criterion (6)–(8).

3. EXPERIMENTAL APPARATUS AND PROCEDURE

The experiments focused on a controlled version of the cigarette smoke phenomenon with which we are all familiar. As shown in Fig. 2, the apparatus consisted of a man-size, airtight, Plexiglas enclosure which was needed to isolate the experiments from ambient air currents present in the laboratory. Two adjacent side-walls and the top and bottom walls of the chamber were constructed of wood. The remaining two adjacent side walls were made of Plexiglas in order to permit the lighting and viewing of the smoke plume.

An axisymmetric air plume was generated above a small heat source placed in the center of the box,

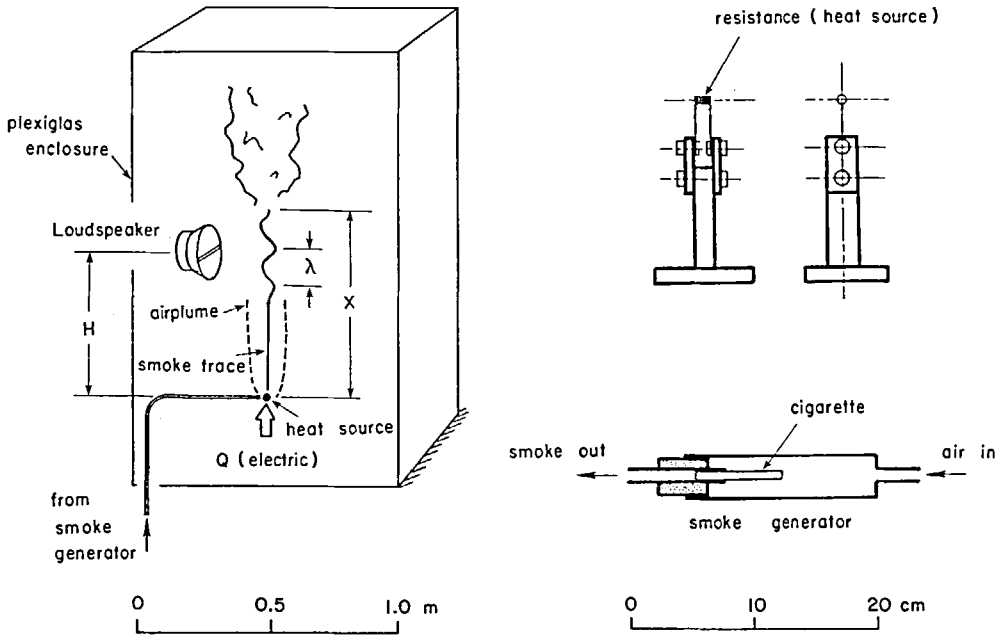


FIG. 2. Schematic of the experimental apparatus.

approximately 45 cm from the bottom. The heat source was constructed in the form of a nichrome resistance coil, as shown in Fig. 2. Electric power in the 0–50 W range was measured and dissipated in the coil: most of this energy was released into the buoyant air plume. (The estimated radiation heat loss was less than 6% at 22 W and less than 20% at 55 W.)

Cigarette smoke was generated in an external device constructed after a design described by Bradshaw [17]. The smoke was released directly beneath the nichrome coil very slowly so that it did not affect the air plume. This simple flow visualization technique worked very well, and the plume shape visualized by the smoke trace was photographed.

The experiments were designed to test the validity of the $t_{\min} \sim t_v$ scaling during transition. For a certain (reference) power dissipated in the coil, Q_0 , the plume shape was photographed 3–6 times. The photographs showed statistically the existence of a characteristic height x_0 and wavelength λ_0 for the beginning of transition (Fig. 2). The power setting Q was changed during the course of experiments and these changes reflected in the measured x and λ . The object of the experiment was to discover the dimensionless functions

$$\frac{x}{x_0} = \text{function} \left(\frac{Q}{Q_0} \right), \quad (9)$$

$$\frac{\lambda}{\lambda_0} = \text{function} \left(\frac{Q}{Q_0} \right). \quad (10)$$

The experimental findings were then compared with the theoretical functions recommended by the $t_{\min} \sim t_v$ scaling. The theoretical functions x/x_0 and λ/λ_0 can be obtained by recalling that the diameter and velocity of a

laminar plume above a point heat source scale as [18]

$$D \sim Q^{-1/4} x^{1/2} \left(\frac{\alpha g \beta}{v^3 k} \right)^{-1/4}, \quad (11)$$

$$U \sim Q^{1/2} \left(\frac{\alpha g \beta}{v k} \right)^{1/2}. \quad (12)$$

At transition we expect $\lambda \sim D$ and $t_{\min} \sim t_v$ [or $D\dot{U}/v \sim \text{constant}$, equation (8)], hence, the theoretical functions to be tested are

$$\frac{x}{x_0} = \left(\frac{Q}{Q_0} \right)^{-1/2}, \quad (13)$$

$$\frac{\lambda}{\lambda_0} = \left(\frac{Q}{Q_0} \right)^{-1/2}. \quad (14)$$

Note that the scaling represented by equations (11) and (12) is valid for Prandtl numbers of $O(1)$ or greater.

4. RESULTS

In the first series of observations the plume was photographed in the absence of any external noise which might act as a trigger for transition. The measured transition heights and wavelengths are shown in Fig. 3: both x and λ decrease as the energy content of the plume Q increases. The variation of λ/λ_0 vs Q/Q_0 parallels the theoretical curve, equation (14) but the measured transition heights are consistently greater than the theoretical levels. Comparing this first series of observations with the theoretical expectations [equations (13) and (14)], we conclude that in the absence of external triggers the transition wavelength scales with the plume diameter, however, the transition is delayed

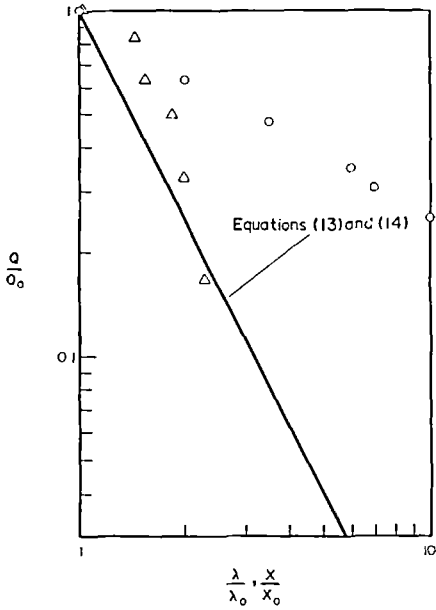


FIG. 3. The transition height and the wavelength as a function of heat input, in the absence of external noise. \circ , x/x_0 , transition height. \triangle , λ/λ_0 , wavelength.

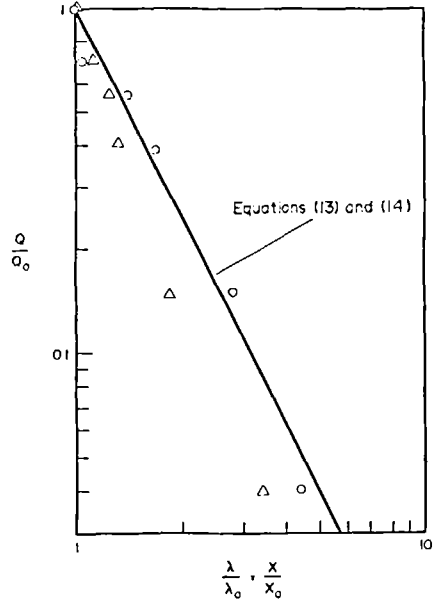


FIG. 4. The transition height and wavelength as a function of heat input. The enclosure wall was tapped by a finger. \circ , x/x_0 , transition height. \triangle , λ/λ_0 , wavelength. $Q_0 = 55 \text{ W}$, $x_0 = 0.25 \text{ m}$, $\lambda_0 = 0.04 \text{ m}$.

and occurs further downstream from the theoretical level.

Considerably more conclusive results were obtained by photographing the plume shapes immediately after tapping the enclosure once, with a finger. This sort of noise served to introduce disturbances of many (unspecified) wavelengths and amplitudes into the air plume flow. Figure 4 shows the measured variation of λ/λ_0 and x/x_0 with Q/Q_0 : the agreement with theory is very good in a relatively wide range of power settings Q/Q_0 . It appears that the stream has the natural ability to filter [19] out of the disturbance spectrum the natural wavelength of transition. The measurements indicate that the natural wavelength scales with the plume diameter (because $\lambda \sim Q^{-1/2}$). These results validate the theoretical basis for adopting $t_{\min} \sim t_v$ as transition criterion (Section 2).

The repeatability of the above observations is demonstrated by the sequence of photographs presented as Figs. 5(a)–(c). These three photographs belong to the same plume, as the plume strength Q was held constant ($Q = 31.1 \text{ W}$). The transition wavelength and height are recorded instantly by means of the vertical scale mounted next to the plume, at the same distance from the camera [note that Figs. 5(a)–(c) were taken at different times, using different focusing lengths]. The photographs show clearly that, given a plume, the transition to non-laminar flow is characterized by a characteristic wavelength λ and a characteristic height x .

The relationship between λ , x and Q at transition (Fig. 4) is illustrated in Figs. 6(a) and (b). From Fig. 6(a) to Fig. 6(b) the source strength Q increases by almost a factor of 2; correspondingly both λ and x decrease by a

factor of the order of $1/\sqrt{2}$ predicted theoretically. Again, transition is characterized by a well-defined ‘meandering’ shape with a unique wavelength and at a unique height.

An important aspect of the plume shape during transition is its two-dimensionality. We investigated this aspect by conducting a separate series of experiments in which the plume was photographed simultaneously from two angles, from the front and from the side. The side-view was visible in a tall mirror placed vertically near the plume, at a 45° angle with respect to the camera-plume direction. The mirror view appears on the LHS of each of the photographs shown in Figs. 7(a)–(c).

By tapping the side of the box once, we had absolutely no control on the plane in which the plume would choose to meander during transition. Thus, we had to take many photographs in order to come across a few cases where the plane of deformation happened to be nearly perpendicular to the camera-plume direction. Two such cases are exhibited in Figs. 7(a) and (b): plume deformation during transition is clearly in one plane. Figure 7(c) shows one of the many cases in which the plane of deformation did not coincide with either the camera-plume direction or with the direction perpendicular to the camera-plume line: regardless of the misalignment, Fig. 7(c) shows that the elbows of the sinusoidal shape are all in the same plane.

The 2-dim., planar, character of the plume deformation during transition [Figs. 7(a)–(c)] is an important conclusion: it contradicts the hydrodynamic stability assumption [13] that the initial deformation (disturbance) in free jet flow is helical (3-dim.).

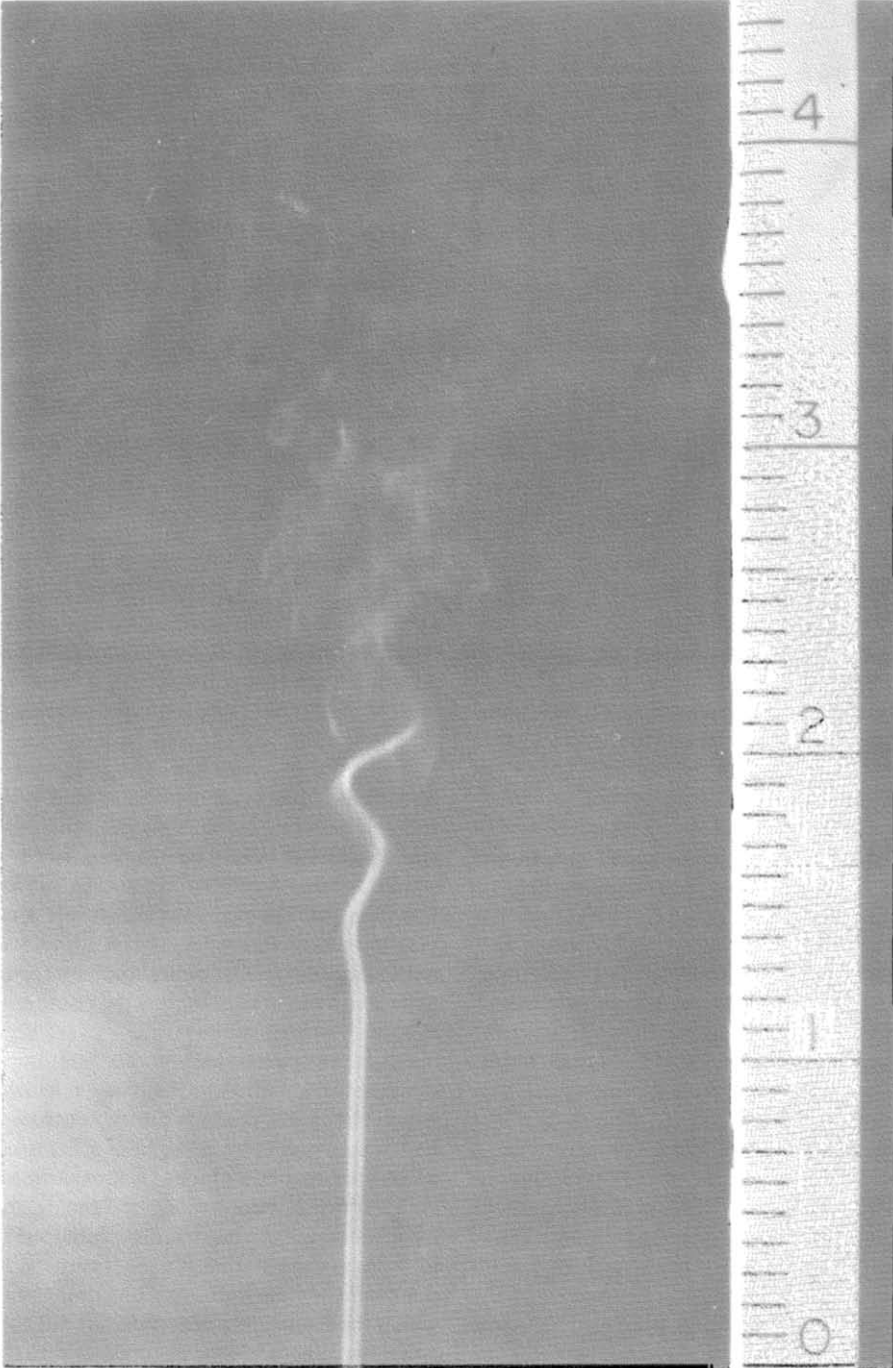


FIG. 5(a).



FIG. 5(b).

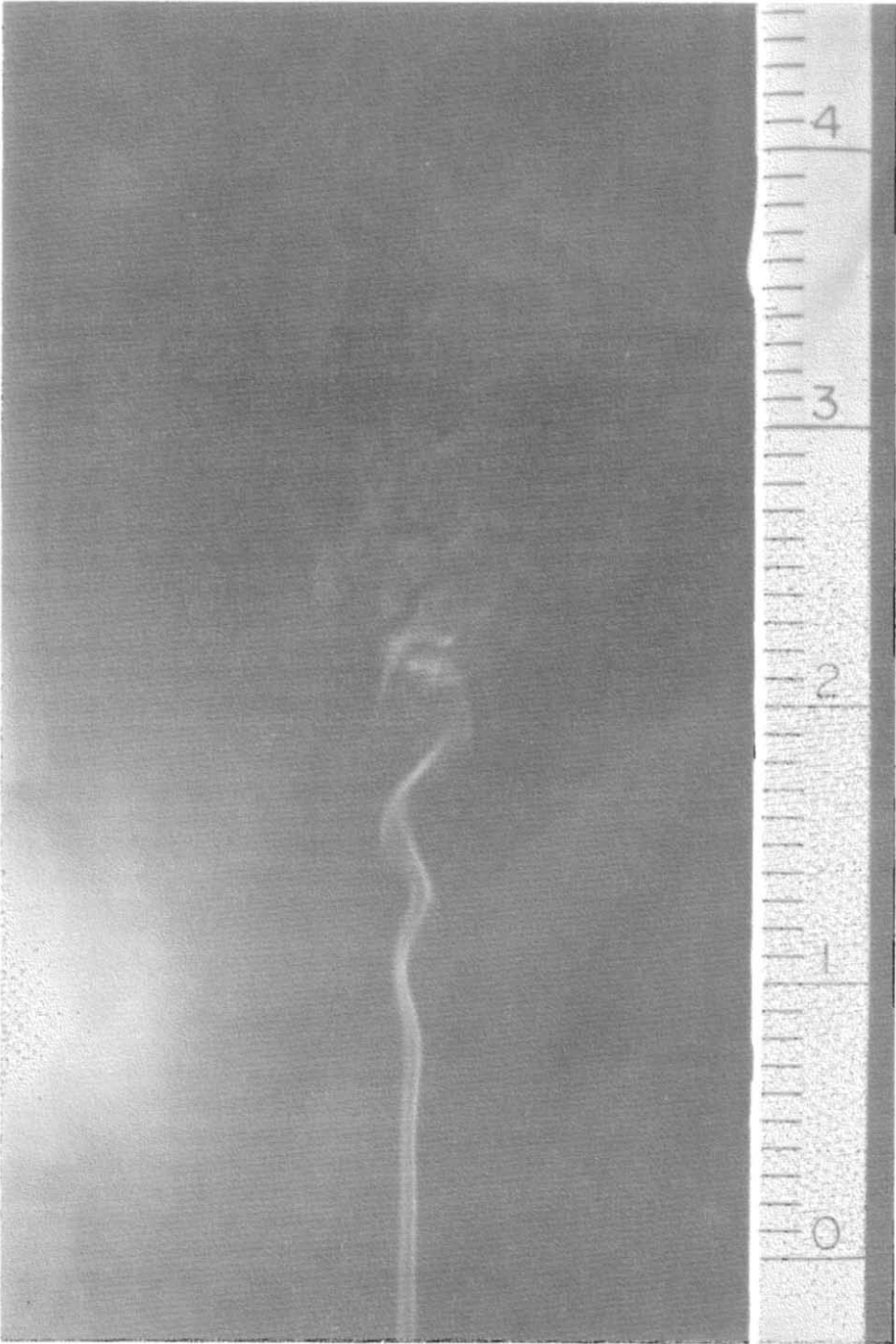


FIG. 5(c).

FIG. 5. Photographs showing the transitional shape of the same plume ($Q = 31.1$ W).

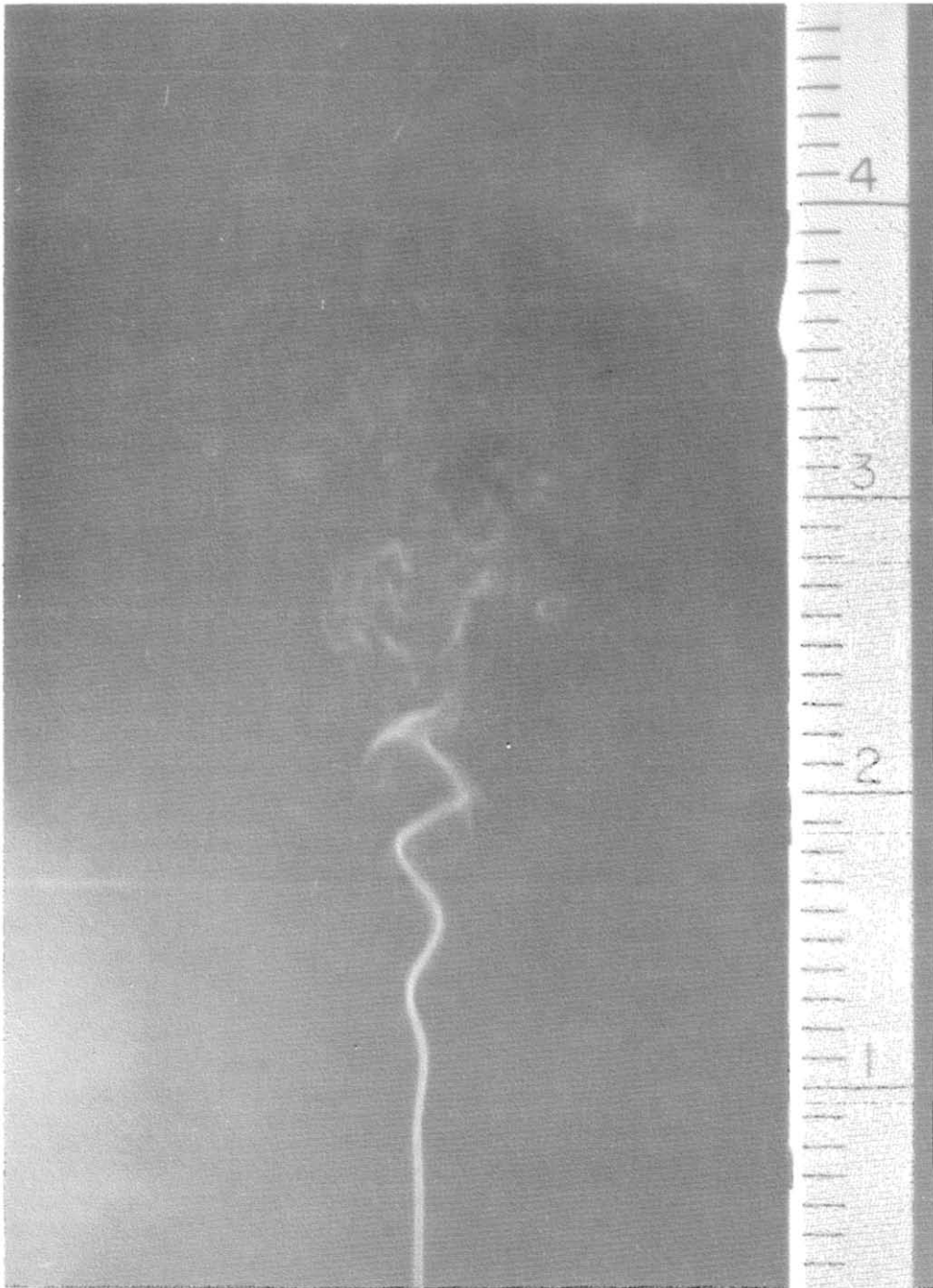


FIG. 6(a). $Q = 21.9$ W.

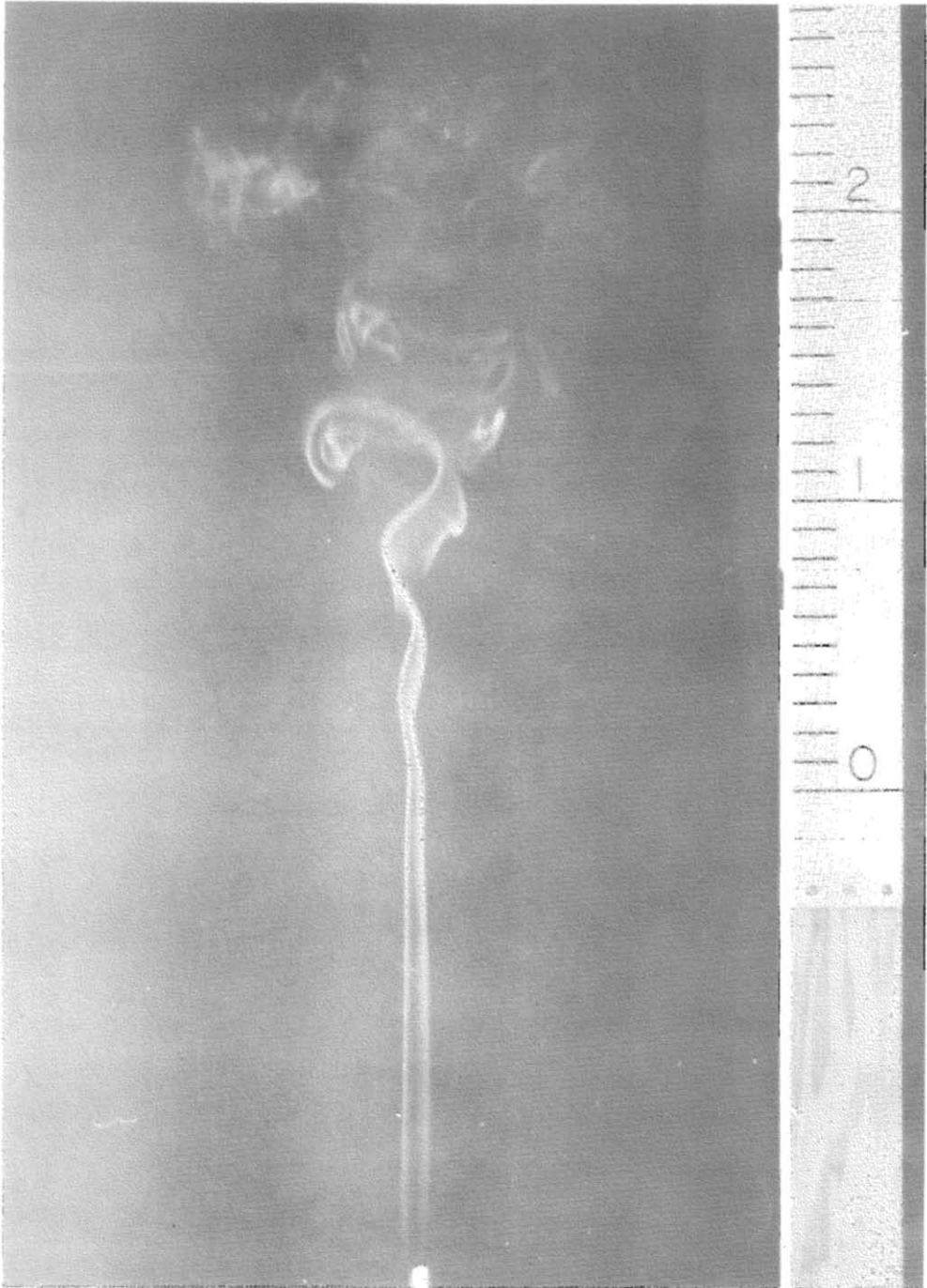


FIG. 6(b). $Q = 38.9 W$.

FIG. 6. The decrease in wavelength and transition height as the plume strength increases.

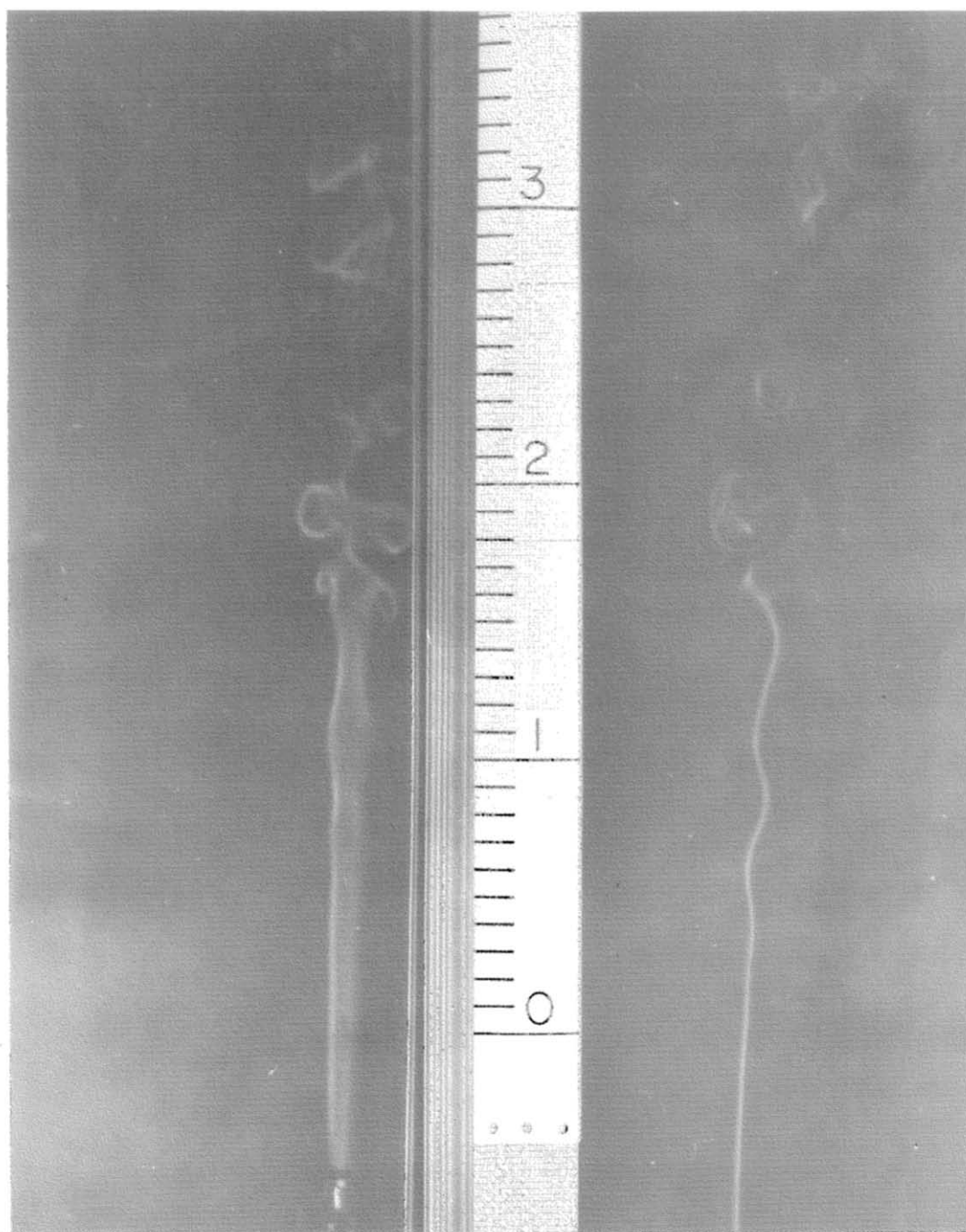


FIG. 7(a). $Q = 5.1 W$.

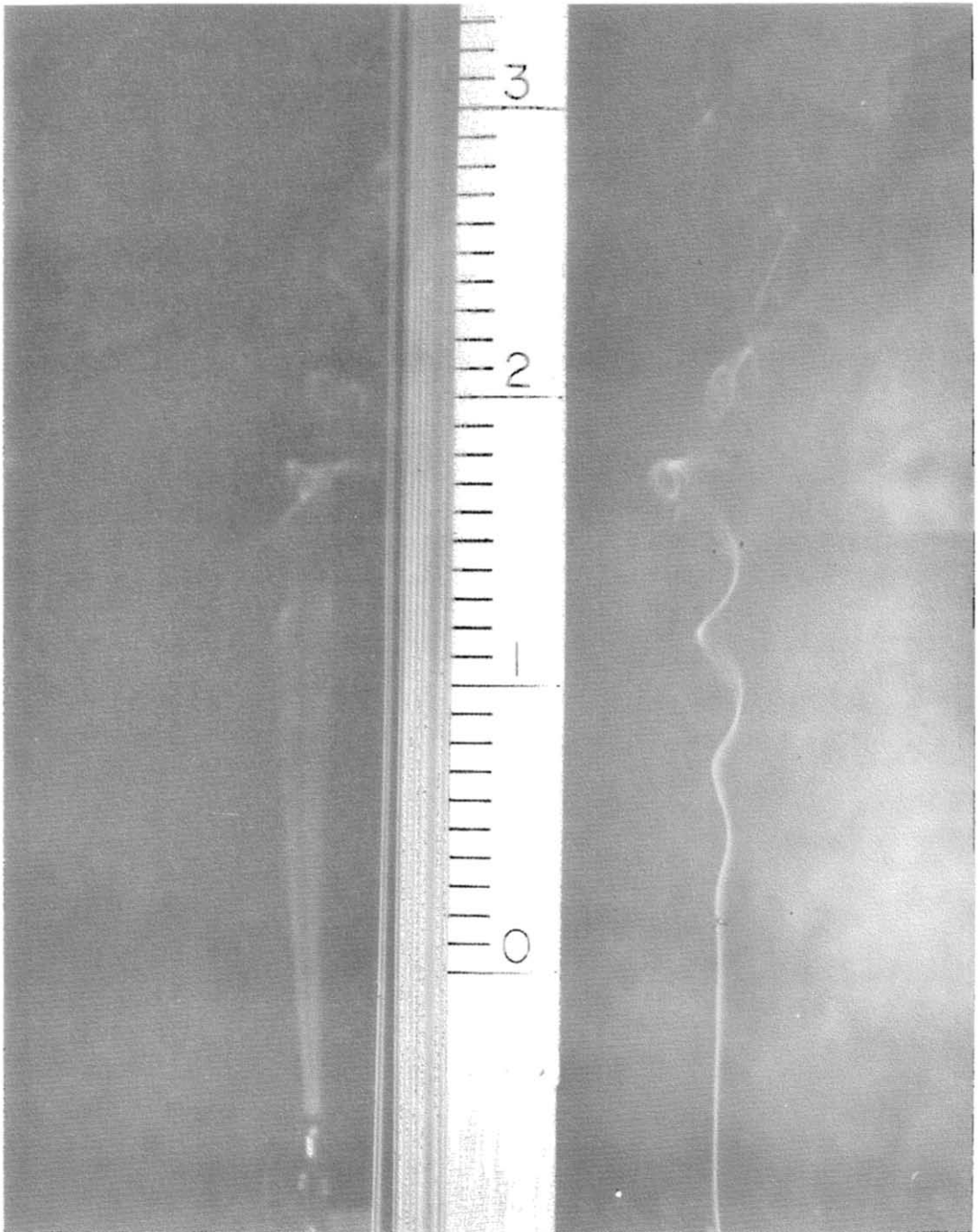


FIG. 7(c). $Q = 12 W$.

FIG. 7. The two-dimensionality of the meandering plume shape during transition.

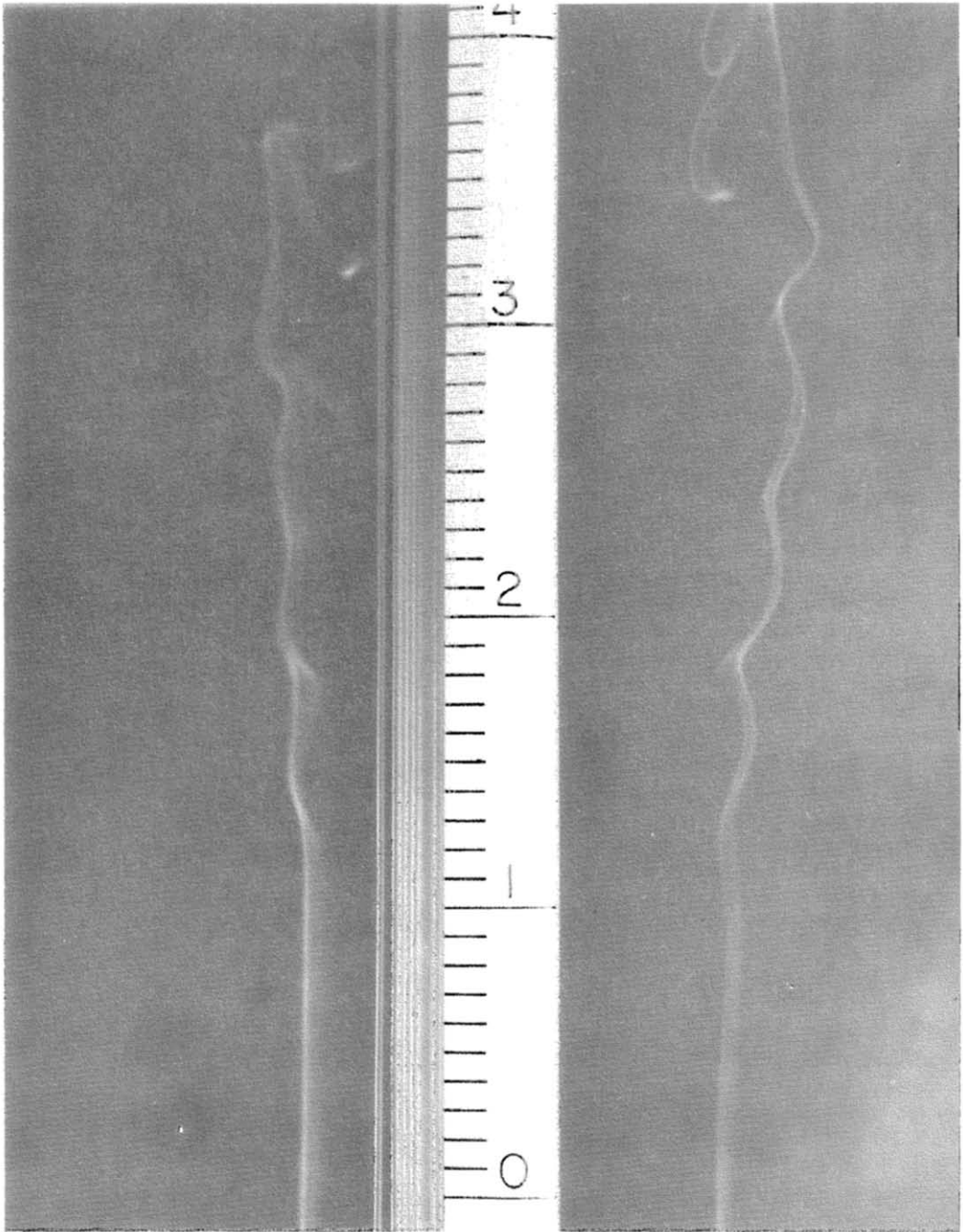


FIG. 7(c). $Q = 12 W$.

FIG. 7. The two-dimensionality of the meandering plume shape during transition.

5. TRANSITION IN A HARMONICALLY-FORCED PLUME

The series of experiments described in the preceding section yielded convincing evidence that the transition phenomenon is the result of the scale properties discussed in Section 2. These properties were studied further in another series of experiments where, unlike in Section 4, the location, intensity and frequency of the 'trigger' disturbance were controlled. The disturbance was generated by a loudspeaker suspended at a certain height, H , next to the plume (Fig. 2). The face of the loudspeaker was covered by a wooden panel with a $3 \text{ mm} \times 200 \text{ mm}$ horizontal slit cut into it. Thus, we were able to harmonically force only a narrow section of the rising plume, at a height determined by the position of the loudspeaker. The intensity of the harmonic forcing (relative to a reference intensity) was monitored by measuring the power needed to drive the loudspeaker.

The experiments were conducted in a manner similar to what led to the observations summarized in Fig. 4. For a fixed heat source strength Q , the plume was disturbed (shaken) at certain frequencies f of the same amplitude (the loudspeaker frequency varied, however, the maximum travel of its cone was held constant). It was observed that the transition height x depended strongly on the frequency of harmonic excitation f . It was found that there exists a characteristic frequency f such that the transition takes place at a minimum height: frequencies higher and lower than this characteristic value triggered transition at higher altitudes. These 'resonance' characteristics have been studied extensively (visually and photographically [20]) and are amply documented in Figs. 8(a)–(f). In Figs. 8(a)–(c) the loudspeaker was held at a level 4.5 cm above the heat source, while in Figs. 8(d)–(f) the loudspeaker height was 13 cm.

The minimum transition height and the corresponding wavelength were found to decrease with the increasing heat source strength Q . These observations are summarized in Fig. 9: they are nearly identical to the results of Fig. 4 obtained by tapping the enclosure once with a finger. Thus, the plume resonates, hence, is deformed most effectively when it is harmonically forced at its natural frequency, with a wavelength that scales with the plume thickness at the transition height.

The acoustic excitation provided by the loudspeaker introduces two more variables in the experiment, the loudspeaker height and the excitation amplitude. In Figs. 8(a)–(f) we show the effect of disturbance amplitude. Increasing the disturbance has the effect of precipitating the transition, i.e. the effect of decreasing the transition height. Raising the loudspeaker from 5.4 cm to 13 cm above the plume origin, has the effect of placing the transition further downstream.

6. TRANSITION REYNOLDS NUMBER GREATER THAN UNITY

As a summary to the preceding series of observations, Fig. 10 shows the actual linear dimensions of

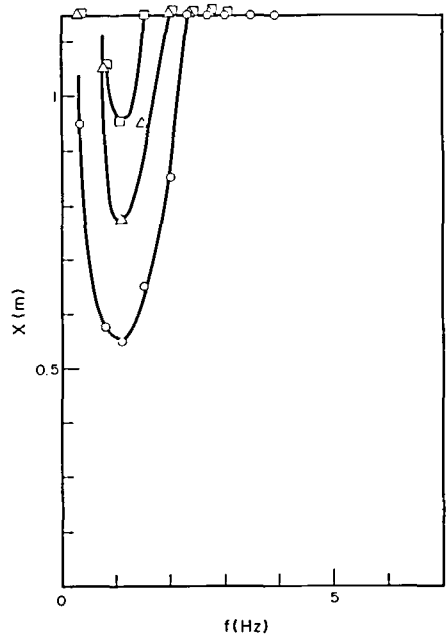


Fig. 8(a). $Q = 1.03 \text{ W}$, $H = 0.045 \text{ m}$. \circ 7V; \triangle 4V; \square 2V.

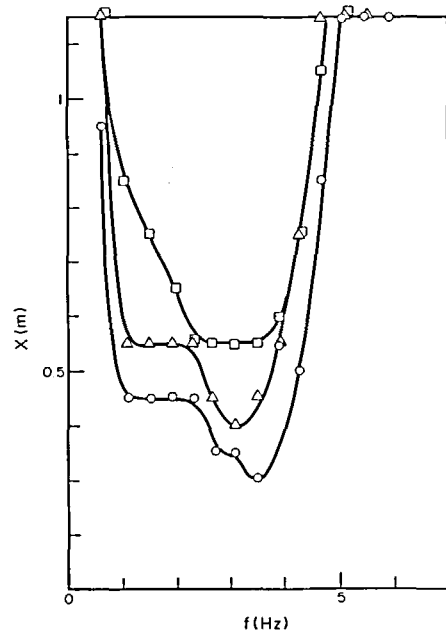


Fig. 8(b). $Q = 4.13 \text{ W}$, $H = 0.045 \text{ m}$. \circ 7V; \triangle 4V; \square 2V.

the characteristic wavelength and transition height (the same measurements are listed in Tables 2 and 3). It is evident that at transition the height x is proportional to the characteristic wavelength λ , in fact,

$$x \sim 10\lambda \quad (15)$$

is an order-of-magnitude fit for the data plotted in Fig. 10. The measured proportionality between x and λ at transition is anticipated correctly by the scaling

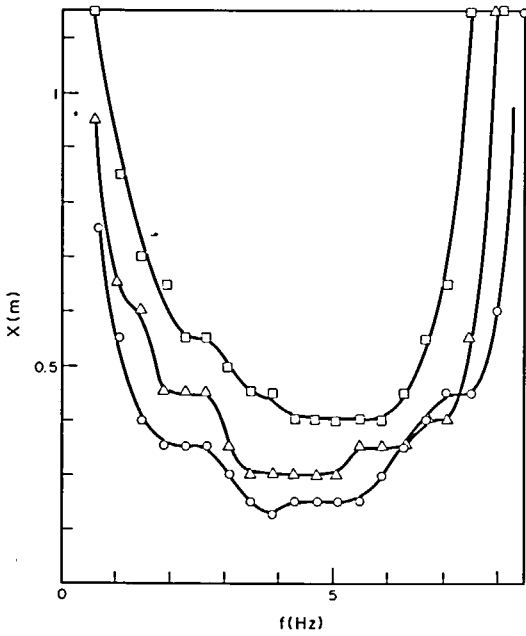


FIG. 8(c). $Q = 8.44$ W, $H = 0.045$ m. \circ 4V; \triangle 2V; \square 1V.

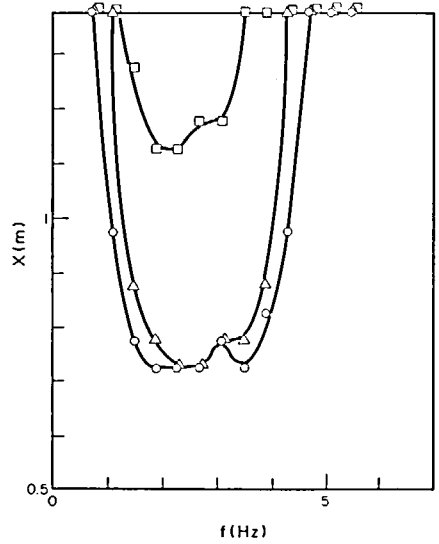


FIG. 8(e). $Q = 4.68$ W, $H = 0.13$ m. \circ 8V; \triangle 4V; \square 2V.

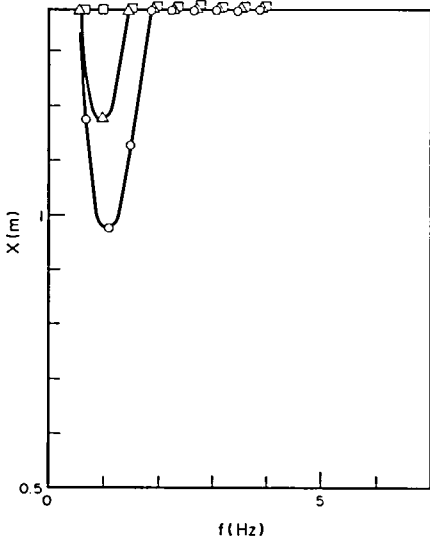


FIG. 8(d). $Q = 1.02$ W, $H = 0.13$ m. \circ 8V; \triangle 4V; \square 2V.

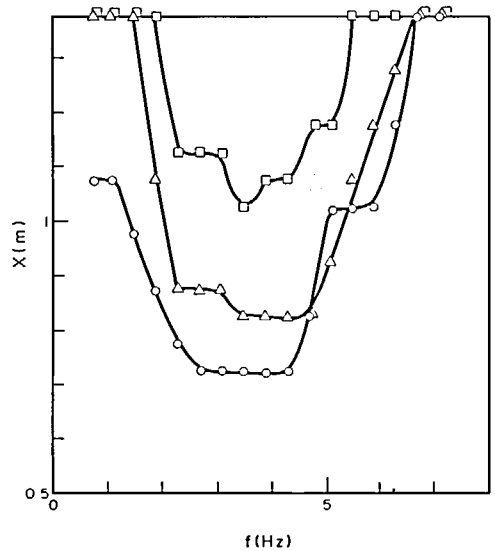


FIG. 8 (f). $Q = 8.5$ W, $H = 0.13$ m. \circ 4V; \triangle 2V; \square 1V.

FIG. 8. Effect of disturbance frequency and amplitude on the resonance characteristics of the plume. The voltage V represents the amplitude of the input signal to the loudspeaker.

argument presented in the beginning of this paper [see equations (13) and (14)].

In addition, note that the coefficient in equation (15) is a number greater than unity. This finding validates the time criterion of transitions, equation (8), which translated into a transition Reynolds number considerably greater than unity. For example, by using the D and U scales of the plume [equations (11) and (12)], the transition height x is eliminated from equation (15)

to obtain

$$\frac{DU}{\nu} \sim 10 \frac{\lambda}{D}. \tag{16}$$

According to Table 1, λ/D can only be of the order of 2 or greater, hence, the transition Reynolds number DU/ν must be a constant considerably greater than unity (in the range $10-10^2$). Thus, the present experimental observations support qualitatively and

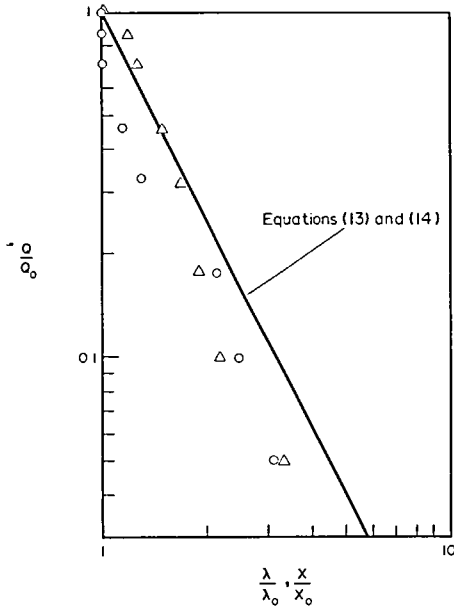


FIG. 9. The transition height and wavelength as a function of heat input, in air plumes excited harmonically by a loudspeaker. \circ x/x_0 transition height; \triangle λ/λ_0 wavelength; $Q_0 = 21$ W; $x_0 = 0.35$ m; $\lambda_0 = 0.06$ m.

quantitatively the transition mechanism envisioned in Sections 2 and 3 and in Fig. 1.

It is worth noting that the local Reynolds number transition criterion $O(N) = 1$ or $DU/\nu = O(10^2)$ stated in equations (6) and (8) and verified above, can be easily translated into the Rayleigh or Grashof number language used in natural convection. In fluids with $Pr > O(1)$ the velocity boundary layer thickness scales as $x Pr^{1/2} Ra^{-1/4}$ and the vertical velocity as $(\alpha/x) Ra^{1/2}$, where Ra is the Rayleigh number $g\beta x^2 Q/(\alpha\nu k)$. Therefore $DU/\nu = O(10^2)$ means that at transition the Rayleigh number is $Ra = O(10^8 Pr^2)$. For the air plumes

Table 2. Transition height and wavelength measurements, plotted in Fig. 4

Q (W)	x (m)	λ (m)
2.0	1.13	0.12
8.6	0.48	0.098
22	0.45	0.049
31	0.35	0.044
39	0.26	0.040
55*	0.25	0.035

* Reference power setting.

considered in our study this prediction reduces to $Gr = O(10^8)$, which is the commonly observed range of transition Grashof numbers (note that $Gr = Ra/Pr$).

7. CONCLUSIONS

This paper described a fundamental study of the phenomenon of transition to turbulence in natural convection plume flow. The experimental part of the study focused on a controlled version of the 'cigarette smoke' plume flow. The experiment demonstrated that:

- (1) at transition, the plume assumes a sinusoidal (meandering) shape of characteristic wavelength, and at a characteristic height above the plume origin [Figs. 5(a)-(c)];
- (2) the transition wavelength scales with the local plume diameter (Figs. 3, 4 and 9);
- (3) the transitional meandering shape is 2-dim., i.e. in one plane [Figs. 7(a)-(c)];
- (4) if the transition is triggered by 'noise', then it is a plume property to 'filter' out of the noise the characteristic transition wavelength which is proportional to the plume diameter at the transition height (Figs. 3 and 4);
- (5) if the transition is triggered by single-frequency forcing, then it is a property of the plume to 'resonate', i.e. to deform most when disturbed with a wavelength which scales with the plume diameter at transition height (Fig. 9).

These experimental conclusions support strongly the theoretical argument presented in Section 2. According to this argument, the phenomenon of

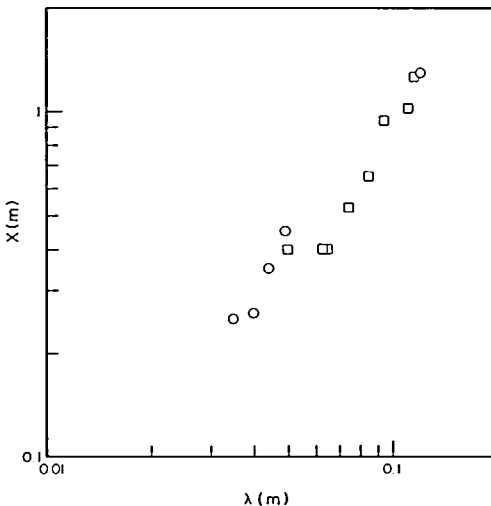


FIG. 10. The measured characteristic wavelength and transition height. \circ data from Table 2; \square data from Table 3.

Table 3. Transition height and wavelength measurements plotted in Fig. 9

Q (W)	x (m)	λ (m)	H (m)	f (Hz)
1.05	1.28	0.15	0.045	1.9
2.13	1.02	0.11	0.045	2.8
3.56	0.94	0.095	0.045	3.9
6.79	0.65	0.085	0.045	5.5
9.7	0.53	0.075	0.045	6.4
14.9	0.40	0.065	0.045	8
17.8	0.40	0.063	0.045	9.1
21.0*	0.40	0.050	0.045	10

* Reference power setting.

transition is:

- (a) an intrinsic property of the flow;
- (b) the result of the internal competition among two characteristic time scales of the stream, the minimum fluctuation period t_{\min} and the viscous penetration time t_v ;
- (c) characterized by a unique meandering wavelength which is always proportional to the local stream thickness.

The transition mechanism proposed in Section 2 evolved from a review of classical hydrodynamic stability results (Table 1) and led to the flow properties (scaling) embodied in the time criterion $t_{\min} \sim t_v$ [equations (6) and (7)]. The same scales and time criterion have been brought to light earlier by the buckling theory of inviscid flow [16]. It was shown recently [21] that the buckling time criterion $N_B = O(1)$ also predicts correctly the transition in free jet flow, shear flow and wake flow, as well as a series of turbulent boundary layer features such as the bursting frequency and the viscous sublayer thickness. Thus, the present study reveals an important relationship (equivalence) between stability theory and buckling theory with regard to explaining transition.

Acknowledgements—This research was supported by the Office of Naval Research.

REFERENCES

1. B. Gebhart, *Ann. Rev. Fluid Mech.* **5**, 213–246 (1973).
2. C. S. Yih, Free convection due to a point source of heat, *Proc. 1st U.S. Natl. Congr. Appl. Math.* **21**, 941–947 (1951).
3. C. S. Yih, Laminar free convection due to a line source of heat, *Trans. Am. Geophys. Un.* **33**, 669–672 (1962).
4. R. S. Brand and F. J. Lahey, The heated laminar vertical jet, *J. Fluid Mech.* **29**, 305–319 (1967).
5. T. Fujii, Theory of steady laminar natural convection above a horizontal line source and a point heat source, *Int. J. Heat Mass Transfer* **6**, 597–606 (1963).
6. K. Brodowicz and W. T. Kierkus, Experimental investigation of laminar free convection flow in air above a horizontal wire with constant heat flux, *Int. J. Heat Mass Transfer* **9**, 81–94 (1966).
7. R. J. Forstrom and E. M. Sparrow, Experiments on the buoyant plume above a heated horizontal wire, *Int. J. Heat Mass Transfer* **10**, 321–331 (1967).
8. A. W. Schorr and B. Gebhart, An experimental investigation of natural convection wakes above a line heat source, *Int. J. Heat Mass Transfer* **13**, 557–571 (1970).
9. L. Pera and B. Gebhart, On the stability of laminar plumes: some numerical solutions and experiment, *Int. J. Heat Mass Transfer* **14**, 975–984 (1971).
10. J. C. Mollendorf, The effect of thermal buoyancy on the hydrodynamic stability of a round laminar vertical jet, Ph.D thesis, Cornell University, Ithaca, New York (1971).
11. Lord Rayleigh, On the stability, or instability of certain fluid motions, *Proc. of London Math. Soc.* **11**, 57–70 (1880).
12. H. Lamb, *Hydrodynamics*, pp. 672–673. Dover, New York (1945).
13. G. K. Batchelor and A. E. Gill, Analysis of the stability of axisymmetric jets, *J. Fluid Mech.* **14**, 529–551 (1962).
14. J. L. Lopez and V. H. Kurzweg, Amplification of helical disturbances in a round jet, *Physics Fluids* **20**, 860–861 (1977).
15. H. Schlichting, *Boundary Layer Theory* (4th edn.), p. 72. McGraw-Hill, New York (1960).
16. A. Bejan, On the buckling property of inviscid jets and the origin of turbulence, *Lett. Heat Mass Transfer* **8**, 187–194 (1981).
17. P. Bradshaw, *An Introduction to Turbulence and its Measurement*, p. 19. Pergamon Press, Oxford (1971).
18. B. Gebhart, *Heat Transfer* (2nd edn.), Ch. 8. McGraw-Hill, New York (1971).
19. B. Gebhart, private communication to A. Bejan, Nov. 1981.
20. S. Kimura, Buckling flow and transition to turbulence in axisymmetric plumes, Ph.D thesis, Department of Mechanical Engineering, University of Colorado, Boulder, Colorado (1983).
21. A. Bejan, *Entropy Generation through Heat and Fluid Flow*, Ch. 4. Wiley, New York (1982).

MECANISME DE LA TRANSITION VERS LA TURBULENCE DANS UN ECOULEMENT DE PANACHE

Résumé—On étudie théoriquement et expérimentalement le mécanisme fondamental responsable de la transition dans la convection naturelle d'un panache. Théoriquement, la transition apparaît quand le temps de pénétration visqueuse normale au panache devient comparable à la période de temps minimale de fluctuation du panache comme un écoulement instable non visqueux. On suppose aussi qu'à la transition, la longueur d'onde du panache est en proportion du diamètre local du panache. La partie expérimentale de l'étude est focalisée sur la transition dans un panache axisymétrique d'air au-dessus d'une source ponctuelle. Une visualisation par fumée de la forme du panache à la transition conduit à des observations extensives qui soutiennent fortement le mécanisme proposé dans la théorie. Le sillage de transition serpente dans un plan (bidimensionnellement) et avec une longueur d'onde qui est à l'échelle du diamètre du panache. S'il est excité extérieurement par des longueurs d'onde, le panache a la propriété de sélectionner la longueur d'onde proposée théoriquement. On discute l'équivalence entre le mécanisme de transition proposé et celui de la théorie du flambement.

DER MECHANISMUS DES ÜBERGANGS ZUR TURBULENZ IN EINER THERMISCHEN AUFTRIEBSSTRÖMUNG

Zusammenfassung—Es wird über eine theoretische und experimentelle Untersuchung der grundlegenden Mechanismen berichtet, die für den Umschlag des Strömungszustandes in thermischen Auftriebsströmungen verantwortlich sind. In der Theorie wird davon ausgegangen, daß dieser Umschlag auftritt, wenn die Zeit für die viskositätsbedingte Durchdringung senkrecht zur Auftriebsströmung vergleichbar wird mit der kleinsten Periode, mit der die Auftriebsströmung im reibungsfreien Fall schwingen könnte. Es wird weiterhin behauptet, daß beim Umschlag die Länge der Stromfahne in einem bestimmten Verhältnis zu ihrem örtlichen Durchmesser stehen muß. Der experimentelle Teil der Untersuchung konzentrierte sich auf den Umschlag in achsensymmetrischen Luftströmungen über einer punktförmigen Wärmequelle. Die Sichtbarmachung der Stromfahne beim Umschlag mit Rauch erlaubte ausgedehnte Beobachtungen der Vorgänge, welche die theoretischen Vorstellungen des Umschlagvorgangs bestärken. Im Übergangsgebiet sieht man, wie die Stromfahne mäanderartige Bewegungen in einer Ebene (zweidimensional) ausführt, wobei ihre Wellenlänge in einem bestimmten Verhältnis zu ihrem Durchmesser steht. Die Strömung hat die Eigenschaft, ihre natürliche, theoretisch vorausgesagte Wellenlänge anzunehmen, wenn sie mit verschiedenen Wellenlängen angeregt wird. Die Gleichwertigkeit zwischen dem vorliegenden Übergangsmechanismus und dem Umschlag nach der "Ausbeulungs"-Theorie wird diskutiert.

МЕХАНИЗМ ПЕРЕХОДА К ТУРБУЛЕНТНОСТИ ПРИ СВОБОДНОКОНВЕКТИВНОМ СТРУЙНОМ ТЕЧЕНИИ

Аннотация—Представлено теоретическое и экспериментальное исследование процесса перехода к турбулентности при свободноконвективном восходящем струйном течении. Теоретически доказано, что переход происходит в том случае, когда масштаб времени вязкого проникновения по нормали к струе оказывается сравнимым с минимальным периодом, при котором струя может пульсировать как неустойчивый невязкий поток. Показано также, что при переходе длина волны струи всегда должна быть связана с локальным диаметром струи. В экспериментах основное внимание было обращено на переход, возникающий в осесимметричной воздушной струе над точечным источником тепла. Дымовая визуализация формы струи при переходе к турбулентности позволила получить большой объем данных, свидетельствующих о справедливости теоретически предложенного механизма перехода. В частности, обнаружено, что в переходном режиме наблюдается характерная длина волны колебаний поля скорости в струе, коррелирующая с диаметром струи. При внешних гармонических воздействиях струя приобретает способность выбирать "естественную" длину волны в режиме перехода, рассчитанную теоретически. Рассмотрено соответствие между предложенным механизмом перехода в свободноконвективной струе и переходом, рассчитанным теоретически.